Articles

Synthesis and Characterization of Hierarchically Ordered Porous Silica Materials

T. Sen,[†] G. J. T. Tiddy,[‡] J. L. Casci,[§] and M. W. Anderson*,[†]

Centre for Microporous Materials, Department of Chemistry, UMIST, Manchester, M60 1QD, United Kingdom, Department of Chemical Engineering, UMIST, Manchester, M60 1QD, United Kingdom, and Synetix, P.O. Box 1, Billingham, Cleveland, TS23 1LB, United Kingdom

Received October 2, 2003. Revised Manuscript Received January 30, 2004

A series of hierarchically ordered porous silica composites were synthesized using anionic (SO_4^{-2}) polystyrene spheres and triblock copolymers Pluronic F127 ($EO_{107}PO_{70}EO_{107}$) and P123 ($EO_{20}PO_{70}EO_{20}$) as templates in the presence of cosurfactants (*n*-alcohols) in an acidic medium. The silica materials were characterized by XRD, SEM, TEM, Hg porosimetry, N_2 adsorption, solid-state NMR, and TG-DTA. At least three distinct pore sizes are observed in these materials. The composites consist of three-dimensional ordered macrospheres (200−800 nm) with interconnecting uniform-sized (70−130 nm) windows. The walls of these macrospheres consist of mesostructured pores (3−8 nm). Nitrogen adsorption indicates the presence of microporosity (<2 nm). Here, we report the detailed synthesis and characterization of such hierarchically ordered porous silica composites (Sen et al. U.K. Patent, GB 0201951.1; *Angew. Chem., Int. Ed.* **2003**, *42*, 4649) with macro−meso−microporous structure and a three-dimensional interconnectivity. These materials could be useful as potential supports for heterogeneous catalysis for bulkier molecules where diffusion of reactant molecules could be facilitated.

Introduction

Porous materials are useful for a variety of applications, for example, heterogeneous catalysis, adsorption, and molecular separation.[1−4] The synthesis, characterization, and applications of microcrystalline porous materials in the microporous range (<2 nm) are well-developed and the subject of much research over the past 3 decades. The synthesis of ordered mesoporous materials with pore sizes above 2 nm was first reported[5] in the early 1990s and has resulted in a vast volume of research over the past decade. Although a full understanding of the formation mechanism is not known, the structure and form are based on the organic−inorganic interface. A surfactant templating route produces such mesoporous materials with a limitation of pore sizes up to 30 nm. The development of ordered porous materials with pore sizes beyond 30 nm (macroporous) is reported for the first time using colloidal templates, for example, polystyrene latex spheres in a colloidal solution[6,7] and oil droplets in an oil-in-water emulsion.[8] Later, various authors have reported the synthesis of macroporous materials using polymer gels,[9] vesicles,[10] foams,[11] and bacteria[12] as templates. These reports demonstrate the synthesis of ordered macroporous materials (>30 nm) with pore sizes on one length scale. These ordered macroporous materials are unlikely to act as a potential support for heterogeneous catalysis due to the low surface area. Introduction of porosity on two or three different length scales in an ordered fashion with interconnectivity between the pores and with hierarchical structure would be advantageous for a variety of applications, for example, catalytic supports, adsorbent, electrode material, slow drug delivery, optics, and electronics. For catalytic applications, where reactant molecules need to access readily the interior pore structure but at the same time where internal surface

* To whom correspondence should be addressed.
[†] Department of Chemistry, UMIST.
[‡] Department of Chemical Engineering, UMIST.
[§] Synetix.

(1) Diddams, P. *Inorganic Supports and Catalysts*; Smith, K., Ed.; Ellis Horwood: New York, 1992; pp 3−39.
(2) Sarrade, S. J.; Rios, G. M.; Carles, M. *Sep. Purif. Technol.* **1998**, *14*, 19.
(3) Nakanishi, K.; Minakuchi, H.; Soga, N.; Tanaka, N. *J. Sol-Gel Sci. Technol.* **1998**, *13*, 163.
(4) Aivasidis, A.; Wandrey, C.; Kiefer, W. U.S. Patent 5,096,814, 1992.
(5) Kresge, C. T.; Leonowicz, M. E.; Roth, W. J.; Vartuli, J. C.; Beck, J. S.; *Nature* **1992**, *359*, 710.
(6) Velev, O. D.; Jede, T. A.; Lobo, R. F.; Lenhoff, A. M. *Nature* **1997**, *389*, 448.
(7) Holland, B. T.; Blanford, C. F.; Stein, A.; *Science* **1998**, *281*, 538.
(8) Imhof, A.; Pine, J. *Nature* **1997**, *389*, 948.
(9) Breulmann, M.; Davis, S. A.; Mann, S.; Hentze, H. P.; Antonietti, M. *Adv. Mater.* **2000**, *12*, 502.
(10) Antonelli, D. M. *Microporous and Mesoporous Mater.* **1999**, *33*, 209.
(11) Sepulveda, P.; Binner, G. P. *J. Eur. Ceram. Soc.* **1999**, *19*, 2059.
(12) Davis, S. A.; Burkett, S. L.; Mendelson, N. H.; Mann, S. *Nature* **1997**, *385*, 420.

10.1021/cm034946u CCC: $27.50
Published on Web 05/06/2004

Table 1. Synthesis Conditions of Anionic Polystyrene Latex Suspensions[a]

batch no.	deionized water (mL)	K-persulfate (g)	stirring speed (rpm)	reaction time (h)	sphere sizes (nm)	solid %
Effect of Water Concentration						
PS-1	1200	0.3315	300	28	230	8
PS-2	1050	0.3315	300	28	312	12
PS-3	900	0.3315	300	28	485	10
PS-4	450	0.3315	300	28	805	14
PS-5	225	0.3315	300	28	857	18
Effect of Stirring Speed and Amount of Radical Initiator						
PS-3	900	0.3315	300	28	485	10
PS-6	900	0.3315	150	28	436	8
PS-7	900	0.4988	300	28	447	6

[a] PS-B8: A commercial sample of polystyrene suspension of size 1 μm from Interfacial Dynamic Corporation.

area is maximized, a ramified pore structure with large pores leading to smaller and then smaller pores is desired. There are many important parameters to be controlled, for example, pore sizes, interconnecting window sizes, pore architecture, ordering of macro- and mesopores (hexagonal, cubic, and lamellar), micropores (zeolitic or dense oxide), and surface area. Stein and co-workers[13] reported one such material with ordered macroporosity and zeolitic wall structure using polystyrene spheres and organic amines as template. The materials exhibited high surface area but poor interconnectivity. Similarly, Kaliaguine and co-workers[14] reported such macroporous materials with mesoporous wall structure (MCM-48). These materials exhibited high surface area due to the mesoporosity but no interconnectivity between the poorly ordered macropores. Stucky, Whitesides, and co-workers[15] succeeded in introducing porosity on three different lengths from macro to meso to micro using stamping of a sol−gel in a silica film. This process is tailored to produce films for optoelectronic application but is not suitable for bulk chemical applications. Our strategy uses synthetic latex spheres to produce a controlled three-dimesionally interconnected macroporosity (300 nm to 1 μm), nonionic block copolymer macromolecular templating to produce mesoscale porosity (ca. 10 nm), and individual polymer templating to produce micropores (ca. 1 nm) in a one-pot synthesis for bulk scale.

Experimental Section

Template Synthesis. Non-crossed-linked, monodisperse polystyrene spheres were synthesized using an emulsifier-free polymerization technique according to the literature.[7] Styrene (105 mL, Fluka, >99% purity) was washed in a separation funnel five times with 100 mL of 0.1 M NaOH (BDH, 99% purity) and then five times with 100 mL of deionized water. After this step the colorless styrene became pale yellow in color and the NaOH solution became pink in color. A five-necked, 2000-mL round-bottom flask was filled with a required amount of deionized water and heated to 70 °C with an isopad isomantle before 100 mL of washed styrene was added. One neck of the flask was attached with stirrer glands (quickfit) connected with a PTFE stirring rod. The stirring rod was connected with an electric motor (Heidolph RZR2051 electronic) having a display of rotation speed. Four other necks were connected with water condenser, thermometer, septum, and pasture pipet connected to a N_2 cylinder with rubber tube. In a separate 100-mL polypropylene beaker, a required amount of potassium persulfate (initiator, Sigma, 99% purity) was dissolved in 50 mL of water and heated to 70 °C. The persulfate solution was added to the reaction flask containing the mixture of deionized water and washed styrene at 70 °C. The whole mixture was stirred at a specific stirring speed for 28 h. The temperature was kept at 70 °C during the reaction. The product was collected through an injection syringe for particle size distribution measurement. The final reaction mixture was milky white and transferred into a polypropylene bottle. The colloidal solution of polystyrene spheres was cooled to room temperature before being stored in a refrigerator at 4 °C. Table 1 presents the effect of water content, $K_2S_2O_8$, and stirring speed of different synthesis batches.

The colloidal spheres were packed into a monolithic structure by centrifugation at 4000 rpm from 30 min to 4 h depending on the size of the spheres. The solid was dried at 60 °C for 2−10 h.

Materials Synthesis. The synthesis of hierarchically ordered porous silica composites were performed using packed polystyrene latex spheres as template and a silica gel containing surfactant and cosurfactant. In a typical synthesis of hierarchically ordered porous materials, 4.06 g of 0.475 (M) HCl was diluted by 9.71 g of deionized water in a polypropylene beaker. Then 18.16 g of tetramethyl orthosilicate (TMOS, Aldrich, purity 99%) was added to the acidic solution. The tetramethyl orthosilicate was vigorously reacted with acidic solution and the temperature of the solution went up to 60 °C. The mixture was stirred by a magnetic needle for 15 min. The temperature of the solution went down to 30 °C while the solution was stirred at RT. A required amount of triblock copolymer, F127 ($EO_{107}PO_{70}EO_{107}$, Sigma) or P123 ($EO_{20}PO_{70}EO_{20}$, BASF), was separately mixed with the required amount of *n*-pentanol (Aldrich, purity 99%) or *n*-butanol (BDH, purity 99%) in another polypropylene beaker. The silica solution was added to the copolymer solution and stirred for another 5 min before addition of 4 g of polystyrene monolith. The whole mixture was stirred for another 15 min before filtration. The filtrate called gel A and the silica gel-filled monolith was called B. Both A and B were dried at 60 °C. The polystyrene latex spheres from B were removed either by direct calcination at 550 °C for 10 h in the presence of air or treatment with toluene followed by calcination at 450 °C for 8 h. The heating rate was 1 °C/min. Nearly 10−15 wt % solid was left after calcination and the calcined materials were white in color. Synthesis was studied by varying three important parameters, for example, the surfactant (P123 or F127), the cosurfactant (*n*-pentanol or *n*-butanol), and the concentration of cosurfactant (*n*-butanol). The compositions of various synthesis batches are presented in Table 2.

Characterization. The presence of long- or short-range ordering in our materials was characterized by powder X-ray diffraction. The X-ray diffractograms were recorded on a XDS

Table 2. Compositions of Various Components during the Synthesis of Hierarchically Ordered Porous Silica Materials

sample name	silica source	surfactant	cosurfactant	macroporous template	pH	temp.(°C)	gel composition (mole ratio)
1B	TMOS	Pluronic F127	*n*-pentanol	PS-3 (485 nm)	1.04	30	F127:H_2O:$C_5H_{11}OH$:HCl:TMOS 0.0032:6.47:0.335:0.01625:1
2B	TMOS	Pluronic P123	*n*-pentanol	PS-3 (485 nm)	1.02	30	P123:H_2O:$C_5H_{11}OH$:HCl:TMOS 0.0068:6.47:0.335:0.01625:1
3B	TMOS	Pluronic F127	*n*-butanol	PS-4 (805 nm)	1.04	30	F127:H_2O:C_4H_9OH:HCl:TMOS 0.0032:6.47:0.335:0.01625:1
4B	TMOS	Pluronic P123	*n*-butanol	PS-4 (805 nm)	1.02	30	P123:H_2O:C_4H_9OH:HCl:TMOS 0.0068:6.47:0.335:0.01625:1
5B	TMOS	Pluronic P123	*n*-butanol	PS-4 (805 nm)	1.03	30	P123:H_2O:C_4H_9OH:HCl:TMOS 0.0069:6.47:0.082:0.016:1

Table 3. Characterization of Hierarchically Ordered Silica Materials[a]

materials	XRD d (nm)	SEM (macropore sizes) pore size, nm (window, nm)	SEM (macropore sizes) thickness (nm)	TEM wall structure, (d_{mac}, nm), (d_{rep}, nm), (t_{meso}, nm), (window, nm)	Hg porosimetry pore opening (nm)	N_2 adsorption S_{BET} (m^2/g)	N_2 adsorption t-plot S_{mi} (m^2/g)	N_2 adsorption V_{mp} (mL/g)	N_2 adsorption V_{mi} (mL/g)	N_2 adsorption d_{mp} (nm)
1B	12.4	290 to 320, (70)	38	line pattern, (344), (10.9), (5.7), (80)	230, 108	179	56	0.16	0.024	4.0
2B	9.1	268 to 315 (no)	82	line pattern, (370), (9.7) (4.7)	290, 72	381	116	0.30	0.050	4.2
3B	10.1	440 to 520 (100)	90	hole structure, (650), (9.9) (1.7), (100)	350, 95	46	11	0.05	0.004	8.2
3B/toluene/cal	8.1	670 (15)	120	hole structure, (595), (7.8) (4.8), (120)	360, 220, 130	531	293	0.19	0.192	3.2
4B	8.9	400 to 480 (115)	51	worm-hole, (600), (8.6) (3.2), (no)	270, 130	89	12	0.10	0.004	6.1
5B	8.3	430 (no)	90	line pattern, (575), (8.8) (3.8) (119)	280, 120	88	7	0.10	0.002	4.9

[a] d_{mac}, macropore diameter; d_{rep}, repeat distance; t_{meso}, mesopore thickness; S_{BET}, total surface area; S_{mi}, surface area due to micropores; V_{mp}, mesopore volume; V_{mi}, micropore volume; d_{mp}, mesopore diameter.

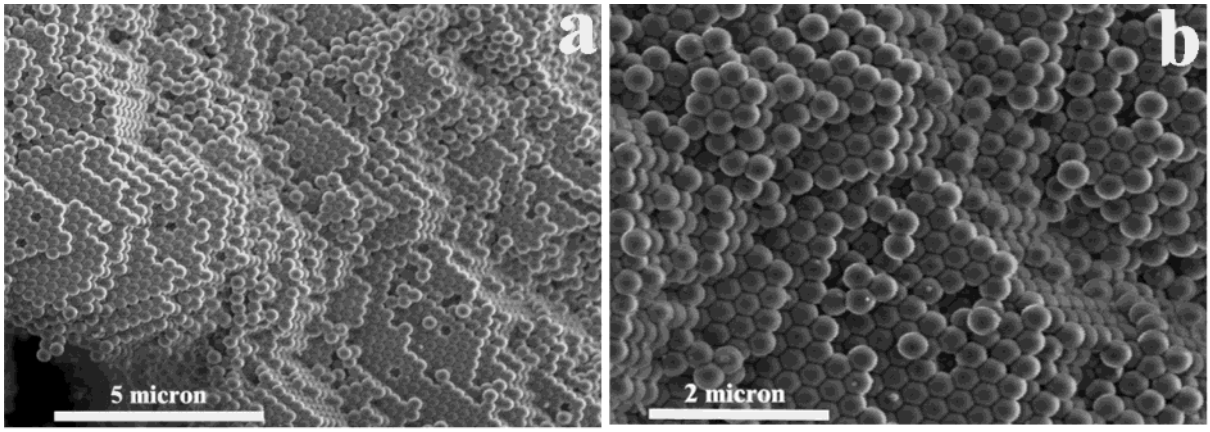

Figure 1. SEM micrographs of PS-2 in two different scales.

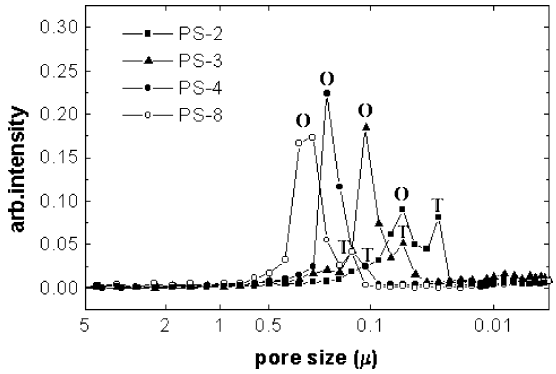

Figure 2. Hg intrusion curves over polystyrene latex spheres of various sizes. O, octahedral; T, tetrahedral interstices sites.

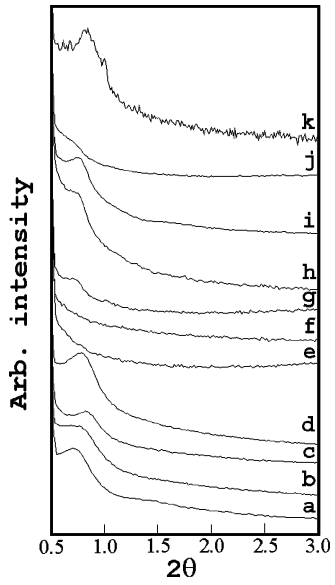

Figure 3. XRD pattern of various samples: (a) 1B, (b) 2B (c) 4B, (d) 5B, (e) 3B/uncalcined, (f) 3B/calcined at 200 °C, (g) 3B/calcined at 300 °C, (h) 3B/calcined at 550 °C, (i) 3B/calcined at 700 °C, (j) 3B/toluene extracted/dried, and (k) 3B/toluene extracted/calcined at 450 °C.

2000 Scintag machine using Cu Kα radiation. All scans were continuous and run between 2θ values of 0.5−10°. The scan rate was 1°/min. The samples were prepared by first drying and then grinding into a fine powder. The powder was then packed into a metal holder, carefully ensuring that the surface was smooth with no visible pits or cracks. The particle size distribution of polystyrene latex spheres in a suspension was characterized by a particle size analyzer (Zetasiser HS100). The particle size, morphology, and macropore structure were characterized by scanning electron microscopy. The scanning electron micrographs were recorded on a Philips XL30 with a field emission gun. The samples were prepared by sprinkling the powder materials onto double-sided sticky carbon films and mounted on a microscope stub and coated with a thin carbon film. Macropores were characterized by a Hg porosimetry experiment using a Micromeritics Autopore IV instrument. The mesopores and the surface area of the materials were characterized by N_2 adsorption using a Micromeritics ASAP2010 instrument. The nature of mesophases and their ordering was further characterized by transmission electron microscopy. The electron micrographs were recorded on a Phillips CM20 200 kV. The specimen for analysis was prepared using a few milligrams of samples crushed and dispersed in acetone. The mixture was then placed onto a copper grid using a dropping pipet. A few drops were used for this preparation. ^{29}Si NMR of various samples was performed on a Bruker MSL 400 spectrometer with magic-angle spinning at a Larmor frequency of 79.474 MHz. The samples were packed inside a rotor and spun at 3-kHz spinning speed. TMS was used as a reference. Simultaneous TG-DTA analyses of the as-synthesized and

(13) Holland, B. T.; Abrams, L.; Stein, A. *J. Am. Chem. Soc.* **1999**, *121*, 4308.
(14) Danumah, C.; Vaudreuil, S.; Bonneviot, L.; Bousmina, M.; Giasson, S.; Kaliaguine, S. *Microporous Mesoporous Mater.* **2001**, *44*, 241.
(15) Yang, P.; Deng, T.; Zhao, D.; Feng, P.; Pine, D.; Chmelka, B. F.; Whitesides, G. M.; Stucky, G. D. *Science* **1998**, *279*, 548.

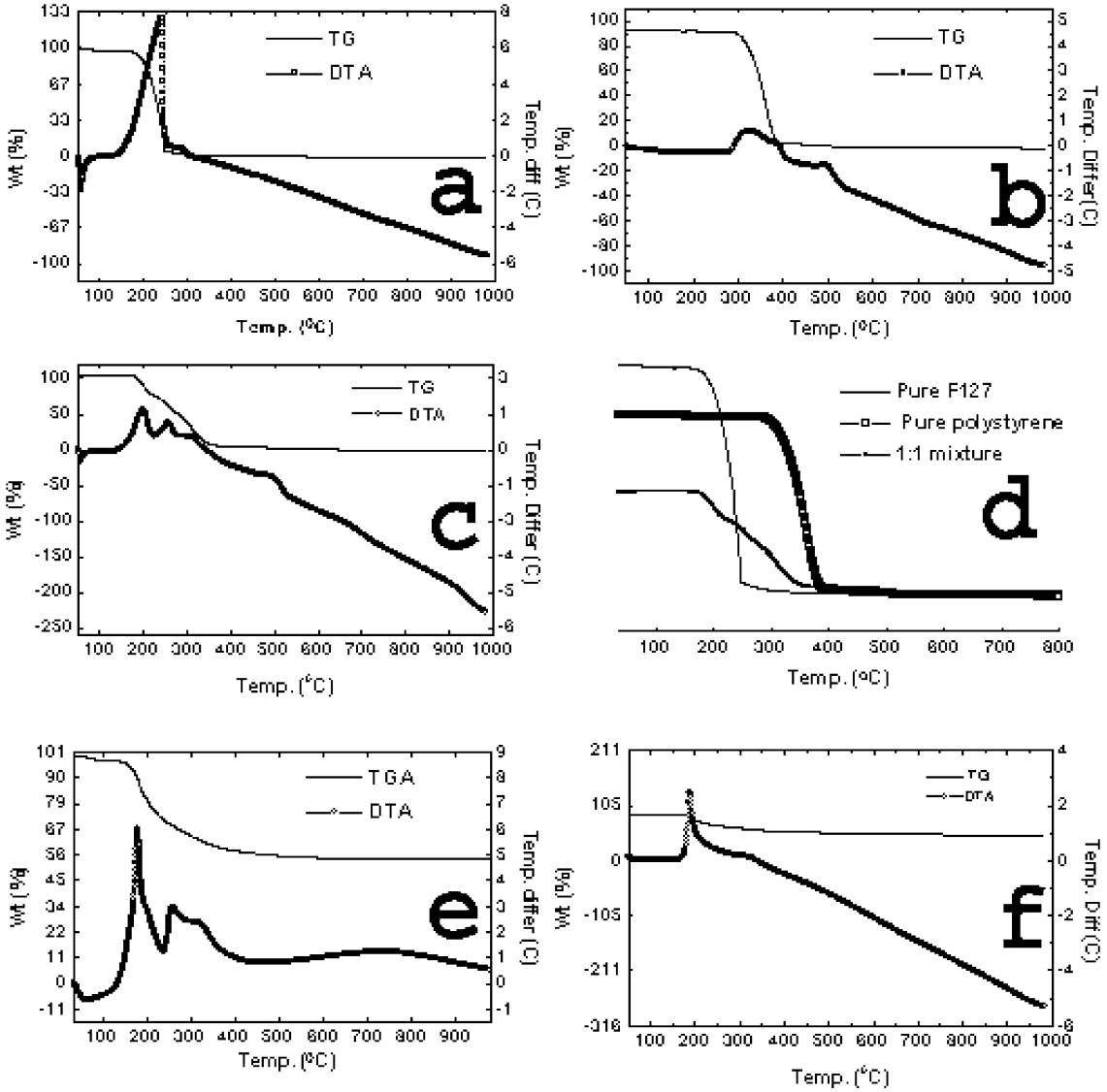

Figure 4. TG-DTA pattern of various samples: (a) Pluronic F127, (b) polystyrene monolith, (c) 1:1 (wt) mixture of Pluronic F127 and polystyrene latex, (d) a comparison of Pluronic F127, pure polystyrene latex, and their 1:1 (wt) mixture, (e) 3B/uncalcined, and (f) 3B/toluene extracted/calcined.

toluene-treated materials were performed on an automatic instrument (TGA-DTA VI.1B TA Inst 2000). The thermograms of the samples were recorded under air (air flow ≅ 16 mL/min) with a heating rate of 5 °C/min.

Results and Discussion

Colloidal Suspension and Packing of Colloidal Particles into a Monolithic Structure. The particle size distribution (from Zetasiser) of polystyrene latex suspensions was narrow with a deviation of ±10 nm. The SEM micrograph of one of the latex samples is presented in Figure 1. The latex particles are spherical in shape with uniform size and form an ordered structure (Figure 1a,b) under centrifugation. The presence of interstitial voids (tetrahedral and octahedral) due to the packing of spheres in the ordered structure is characterized by Hg porosimetry. In this experiment, the Hg is pumped through the sample from normal pressure to 60000 psi to measure the Hg intrusion due to the pores of size ranging from few hundred micrometers to 6 nm. Figure 2 presents the incremental intrusion over four different polystyrene monoliths. It is clearly observed that two types of pore openings are present over all monoliths. The position of the peaks shifted toward larger pore sizes with increasing of the sphere sizes. The positions of the peaks match closely with those expected for O_h and T_d interstices sites calculated from radius ratio rules. The total uptake of Hg corresponds to the void volumes due to the T_d and O_h interstices sites. The sharp increase of cumulative intrusion at 0.1 μm (see Supporting Information) indicated the narrow pore size in this region. The monoliths were stable upon Hg intrusion as there was a sharp decrease of Hg in the extrusion cycle. The monolithic structure of the polystyrene latex spheres was destroyed when a pressure of ~23000 psi was applied for 2 min (see Supporting Information). The monolith completely collapsed in acidic and basic solution when dried at 100 °C (see Supporting Information).

Hierarchically Ordered Porous Materials. All samples exhibited a broad diffraction reflection in the region of 2θ from 0.6° to 1.1° (Figure 3). The maximum and minimum d values are 12.4 nm for 1B/calcined (Figure 3a) and 8.3 nm for 5B/calcined (Figure 3d). The

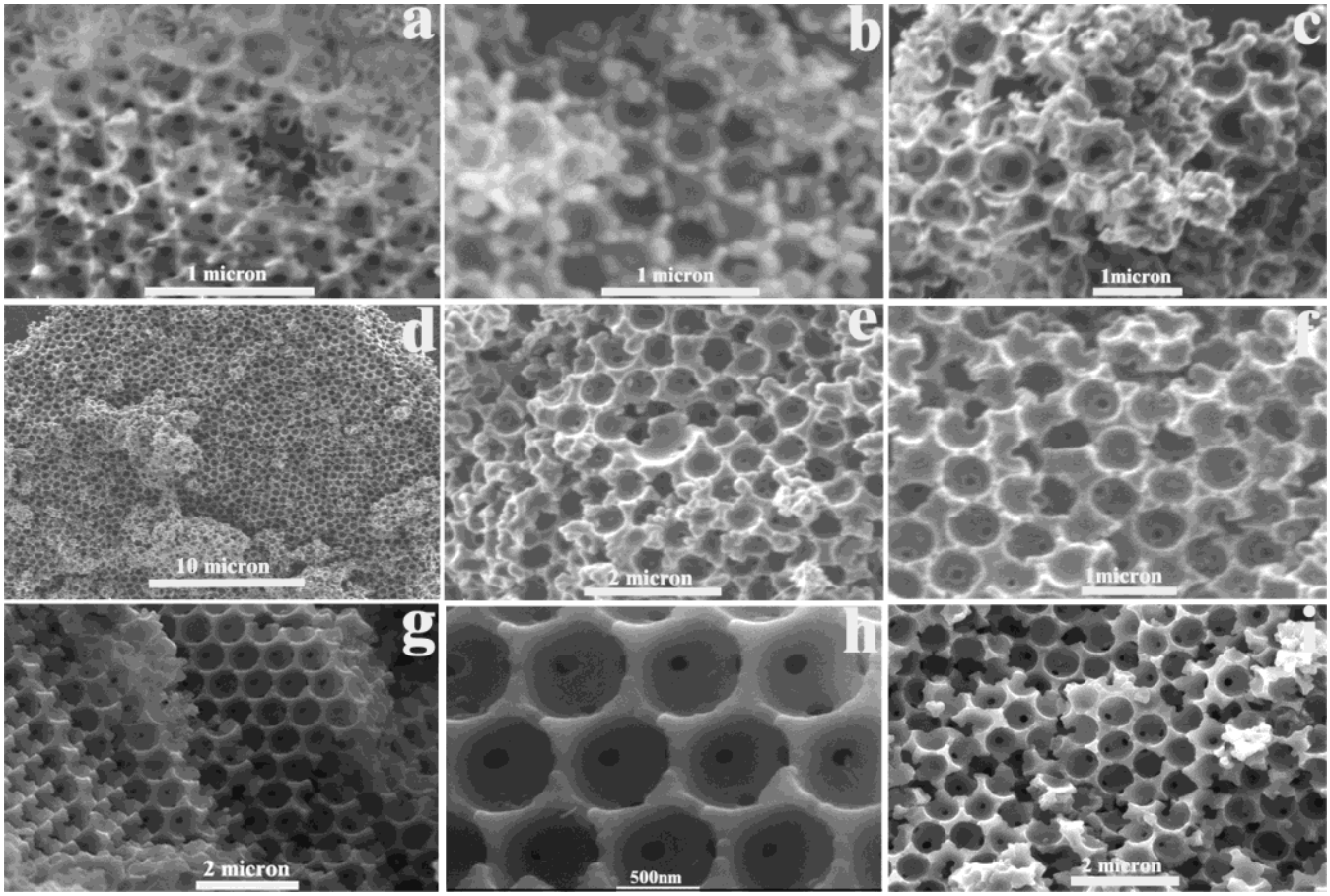

Figure 5. SEM micrographs of silica samples: (a) 1B/calcined, (b) 2B/calcined, (c) 4B/calcined, (d) 5B/calcined, (e) 3B/calcined, (f) 3B/toluene extracted/calcined, (g and h) 3B/toluene extracted/dried in two different scales, and (i) 3B/toluene extracted second time/dried.

effect of template removal by calcination or solvent extraction was studied in 3B. The XRD patterns of 3B were systematically collected over samples calcined at different temperatures (200, 300, 550, and 750 °C). It is observed that the uncalcined (Figure 3e) and the sample calcined at 200 °C (Figure 3f) exhibited no low-angle peaks. This may be due to the low silica concentration in the sample or the absence of mesophase. The sample calcined at 300 °C (Figure 3g) and 550 °C (Figure 3h) exhibited low-angle peaks at $d = 9.7$ and 10 nm due to the removal of polystyrene latex. The peak position at $d = 10$ nm of the calcined material is consistent with the XRD result of 3B ($d = 10.1$ nm, Table 3). Upon removal of polystyrene latex by toluene treatment, sample 3B/toluene exhibited a low-angle peak at $d = 10$ nm (Figure 3j) but shifted to 8.1 nm (Figure 3k) due to calcination at 450 °C. This result suggests that the mesopore size of the solvent-extracted sample (3B/toluene extracted/calcined) is smaller than the directly calcined sample (3B/calcined). Changing the surfactant from F127 to P123 decreases the *d* spacing from 12.4 to 9.1 nm of the mesophases (Figure 3a,b). Similarly changing the cosurfactant from *n*-pentanol to *n*-butanol decreases the *d* spacings from 12.4 to 10 nm of the mesophase (Figure 3a,h). The *d* spacing increases from 8.2 to 8.9 nm by decreasing the cosurfactant concentration (Figure 3c,d). The mesophase is stable even upon heating the sample 3B at 750 °C (Figure 3i). There is a small shift in the *d* spacing due to heating at high temperature.

To understand the calcination step, TG-DTA experiments were performed on various pure samples, for example, pure surfactant F127 (Figure 4a), pure polystyrene monolith (Figure 4b), and a 1:1 mixture of surfactant and polystyrene monolith (Figure 4c). The surfactant F127 burned completely below 250 °C whereas polystyrene burned completely at 500 °C. The small endothermic peak below 100 °C is due to the loss of water whereas the presence of exothermic peaks at 240 °C (pure F127) or 323°, 383°, and 496 °C (pure polystyrene) are due to the burning of F127 and polystyrene spheres. The amount of weight loss for individual components calculated from TG-DTA results is similar to the composition of the mixture (weight ratio 1:1). It is observed from Figure 4c that the positions of the exothermic peaks in the mixture were shifted to lower temperature (199, 260, 370, and 495 °C). This could be due to the simultaneous burning of the surfactant and polystyrene. The mixture was completely burnt at relatively low temperature (<400 °C) in comparison to the pure form and the result is presented in Figure 4d.

The TG-DTA of 3B was performed under the same conditions as above and is presented in Figure 4e. The total weight loss for the uncalcined sample is around 90% due to the burning of polystyrene and surfactant F127. The exothermic peak at 286 °C is due to the burning of the surfactant (weight loss ∼ 20%). The remaining weight loss (∼70%) is due to the burning of polystyrene, resulting in exothermic peaks centered at 352, 368, and 537 °C. Upon toluene extraction, the

weight loss was around 45% (Figure 4f). The amount of surfactant left after the toluene extraction was nearly the same (20%) as the uncalcined sample. This is due to the fact that the surfactant is not removed by toluene extraction whereas nearly 50 wt % of the polystyrene is dissolved out by solvent extraction. The exothermic peak at 198 °C may be due to the catalytic decomposition of surfactant at low temperature in the presence of silica.[16] The exothermic peaks at 270 and 308 °C may be due to the burning of polystyrene spheres. No weight loss is observed after 400 °C. Hence, the toluene-treated sample was calcined at 450 °C.

The macropores (>50 nm) of various samples were characterized by SEM. All samples exhibited a honeycomb structure (Figure 5) with or without interconnecting windows. The window sizes and wall thickness were measured from SEM micrographs and are presented in Table 3. The calcined form of 1B, 3B, 4B, and 3B/toluene exhibited interconnecting windows between the macrospheres whereas 2B and 5B exhibited no interconnecting windows. The interconnecting windows are clearly visible when the polystyrene was removed by toluene extraction (Figure 5g−i). The size of the macrospheres corresponds well to the size of the polystyrene spheres used as template. Twenty to thirty percent contraction in macropore size is observed in all samples due to the removal of polystyrene latex by calcination.

XRD patterns of various samples indicated the presence of a mesophase without any indication of special ordering. The mesophase and detailed macrostructure were further characterized by TEM. The TEM images of one set of calcined samples (1B and 2B) are presented in Figure 6. Sample 1B exhibits a line pattern with spacing of 12 nm whereas 2B/calcined exhibited a disordered mesostructure. The windows are clearly visible in the TEM image of 1B/calcined. The size of the macrospheres, window sizes, mesopores size, and wall thickness of mesopores are presented in Table 3. The TEM images of the calcined form of 3B and 5B are also presented in Figure 7. 3B and 5B exhibited an ordered mesophase with hole and layer structure, respectively. The repeat distance calculated from TEM images (Figure 7b,d) are around 9.9 and 8.8 nm. These values correspond well to the reflections observed from powder XRD (see Table 3). The window size measured from the TEM image (100 nm for 3B) corresponds well to the result obtained from SEM micrographs. An amorphous region is clearly visible around the windows (Figure 7a). 4B/calcined exhibited an ordered macrostructure without any ordering on the mesoscale (see Supporting Information). The microporosity is not observed in the TEM, owing to its disordered nature.

Hg porosimetry was used for the first time to understand the macropore structure and pore interconnectivity in this type of material. The cumulative and incremental intrusion was plotted against pore diameter and the results are presented in Figure 8. The Hg intrusion in the low-pressure region (large pore diameter >100 μm) is due to the interparticle voids (not shown) whereas Hg intrusion due to the high-pressure region (small pore diameter) was due to the interconnecting windows between macrospheres. The total

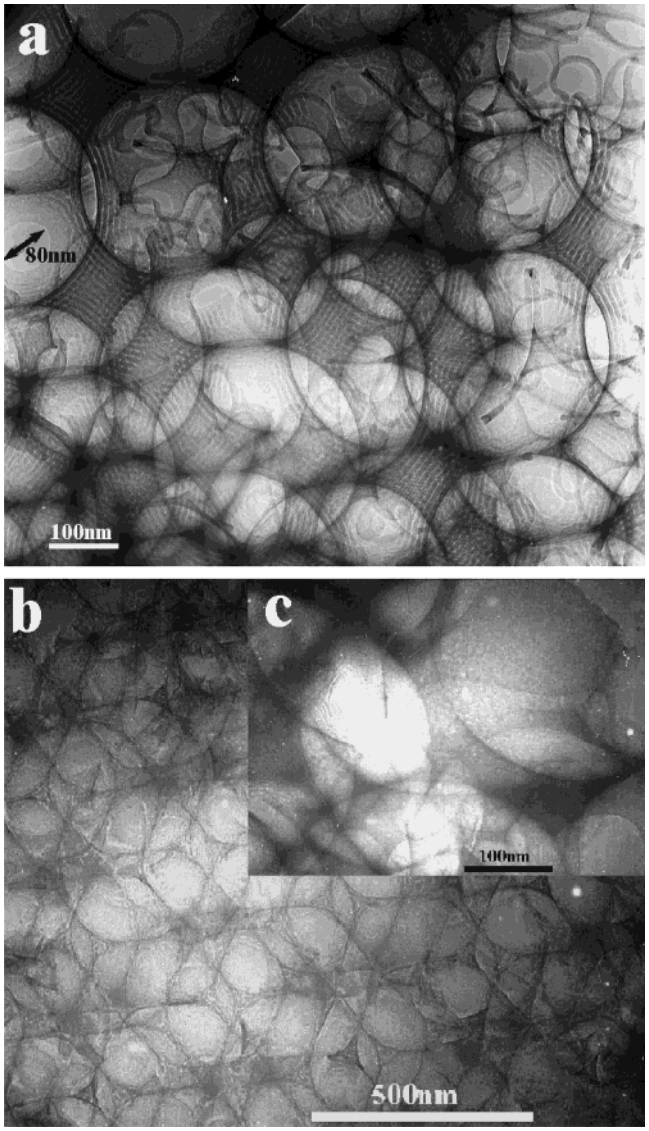

Figure 6. TEM images of 1B/calcined (a) and 2B/calcined (b) and enlarged part of "b" (c).

intrusion (at inflection point) of Hg (Figure 8a,c) by calcined materials 1B and 2B is nearly the same (~3.4 mL/g) with a bimodal pore size distribution (230 and 108 nm and 290 and 72 nm). This result supports the interconnectivities of macrospheres in these materials. Similarly, the Hg porosimetry of another set of calcined samples (3B, 4B, and 5B) are presented in Figure 10e−j. Total Hg intrusion of various calcined samples (3B, 4B, and 5B) is nearly the same and the value is around 3.2 mL/g. The pore size distribution is mostly a bimodal type. The pore openings of three different samples are 350 and 95, 270 and 130, and 280 and 120 nm, respectively. The presence of interconnecting windows is identified through Hg intrusion where a combination of SEM and TEM is necessary to identify the windows of 4B and 5B samples.

The formation of macrospheres by polystyrene latex templating was systematically carried out on 3B. Figure 9 presents the cumulative and incremental intrusion of Hg vs pore size over 3B samples starting from the uncalcined sample to calcined sample at various temperatures. The starting monolith PS−B4 (sphere size = 805 nm) had a bimodal Hg intrusion of sizes 180 nm

(16) Zhao, D.; Huo, Q.; Feng, J.; Chmelka, B. F.; Stucky, G. D. *J. Am. Chem. Soc.* **1998**, *120*, 6024.

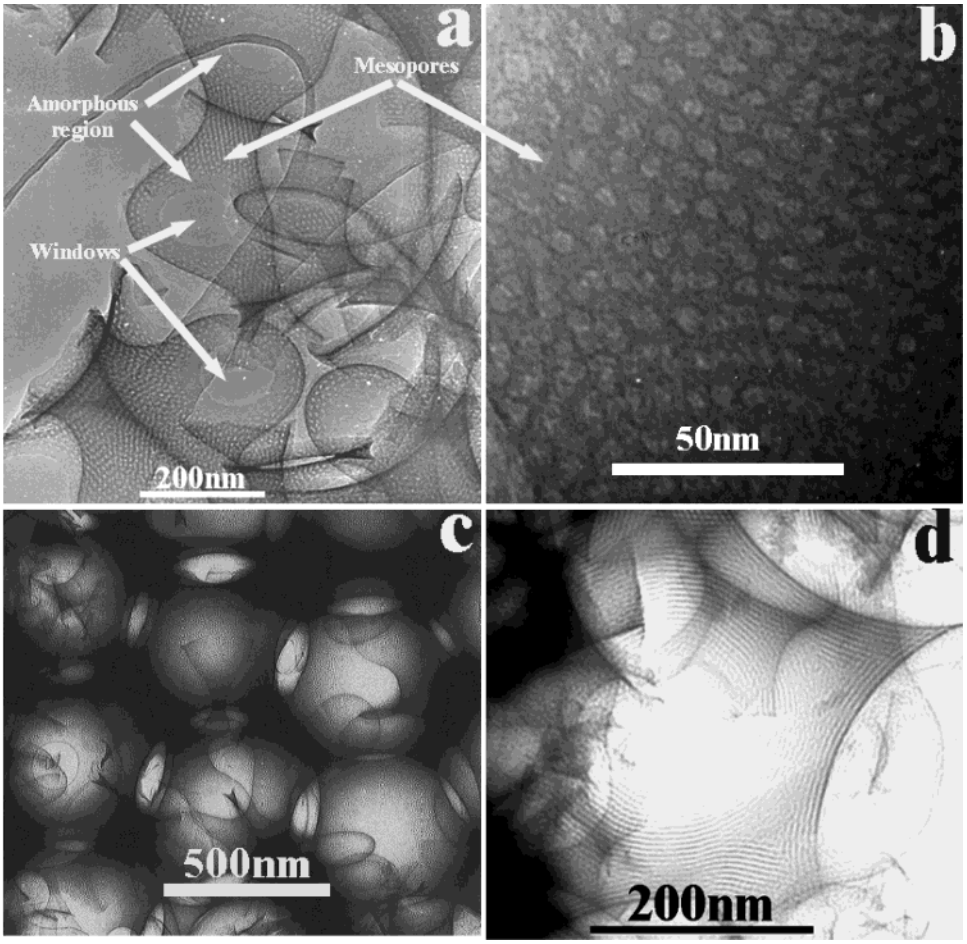

Figure 7. TEM images of 3B/calcined (a), enlarged part of "a" (b), 5B/calcined (c), and enlarged part of "c" (d).

(0.4 mL/g) and 99 nm (0.08 mL/g). The Hg intrusion became unimodal over 3B/uncalcined. The total intrusion due to the pore of 180 nm was half (0.23 mL/g). It indicates that tetrahedral interstices sites are completely filled and nearly 50% void volume due to octahedral interstices sites was still unfilled. The Hg intrusion became nil when the material was calcined at 200 °C. This is due to the absence of void volume because of melting of polystyrene spheres at 200 °C. There was a multimodal distribution (1600, 810, 350, 180, and 97 nm) in Hg intrusion when the material was calcined at 300 °C. The total intrusion was 1.6 mL/g. The sample calcined at 550 °C again produced a bimodal pore distribution (290 and 97 nm). The total intrusion was 3.2 mL/g due to the presence of macrospheres. This study shows that the macropores start to form after the polystyrene latex melts at 200 °C. The formation of macropores above the melting point of latex is not straightforward as there are many simultaneous processes occurring during the calcination, for example, melting of polystyrene latex, burning of surfactant, and burning of polystyrene latex.

The mesopores were further characterized by N_2 adsorption (Figures 10 and 11). All samples exhibited a type IV isotherm having an hysteresis loop (type H2). The BET surface area of these materials is not high in comparison to those of pure mesoporous or microporous materials. The low values may be due to the thin mesoporous walls in these hierarchical structures. The surface area of material 3B/calcined was very low (46m^2/g) without any hysteresis in the adsorption isotherm. The surface area and mesopore volume decreased after toluene treatment but increased up to 12- and 6-fold after calcination of the toluene-treated sample (Figure 11b, Table 3). This result clearly shows that Pluronic F127 does not dissolve out by toluene treatment. This is consistent with the result obtained from TG-DTA (original 20% surfactant remained after toluene treatment). The low surface area and mesopore volume is due to restricted access of N_2 inside the mesopores in the presence of surfactant Pluronic F127. Upon calcination at 450 °C of the toluene-treated sample, high surface area (531 m^2/g) and mesopore volume (0.19 mL/g) were achieved. The mesopores are, therefore, free from surfactant and N_2 can enter the mesopores along with additional micropores created due to the removal of EO groups from the mesoporous walls during the calcination. The total surface area (S_{BET}) is a combination of the microporous and mesoporous surface area. The presence of micropores in this sample is evident from the observation of a large N_2 uptake (Figure 11b) at low p/p_0 (<0.1) and a positive slope in the *t*-plot (Figure 11d). *t*-Plot analysis is a routine method[17] to characterize microporous materials; however, it becomes complicated in the presence of different porosities. Recently, Fajula and co-workers[18] have reported the

(17) Sing, K. S. W. *Chem. Ind.* **1968**, 1520.
(18) Galarneau, A.; Cambon, H.; Di Renzo, F.; Fajula, F. *Langmuir* **2001**, *17*, 8335.

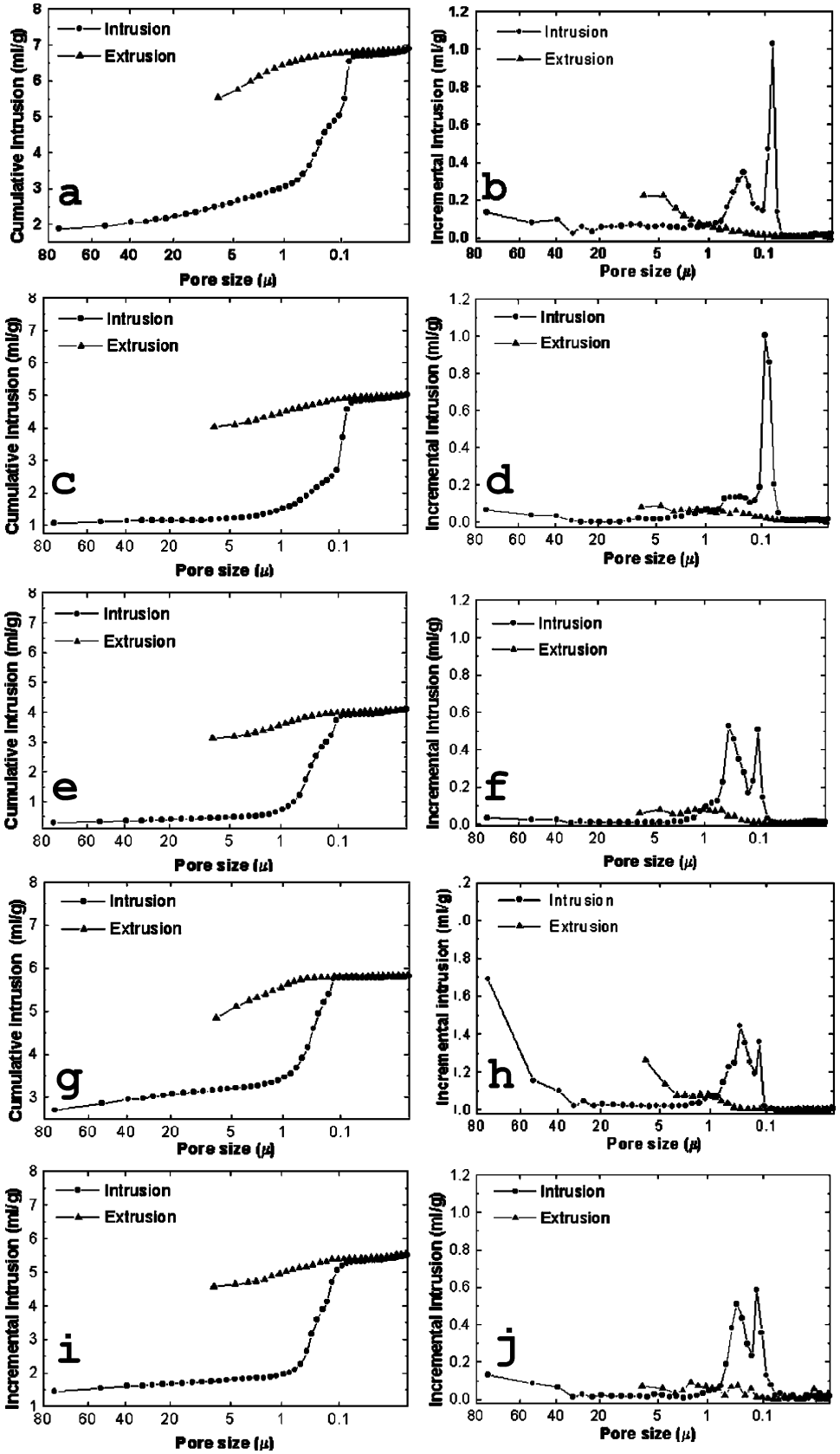

Figure 8. Hg porosimetry results of various samples: (a and b) 1B/calcined, (c and d) 2B/calcined, (e and f) 3B/calcined, (g and h) 4B/calcined, and (i and j) 5B/calcined.

presence of microporosity in mesoporous materials (MCM-41 and SBA-15) by *t*-plot analysis. SBA-15 (synthesized using triblock copolymer as template) exhibited *t*-curves that do not pass through the origin, showing distinct microporosity, with a micropore volume classically determined at the intercept with the *Y*-axis. Similarly our materials exhibited *t*-plot with positive slopes with downward deviation that strongly suggest

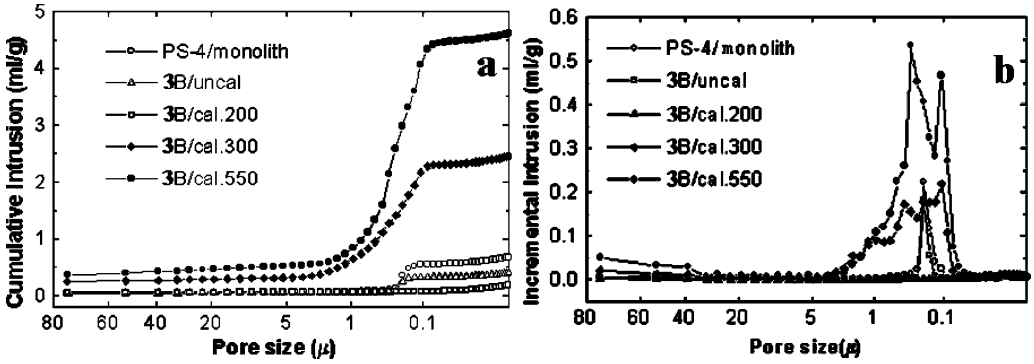

Figure 9. Cumulative (a) and incremental (b) intrusion of Hg in 3B calcined at various temperatures along with polystyrene latex monolith PS-4.

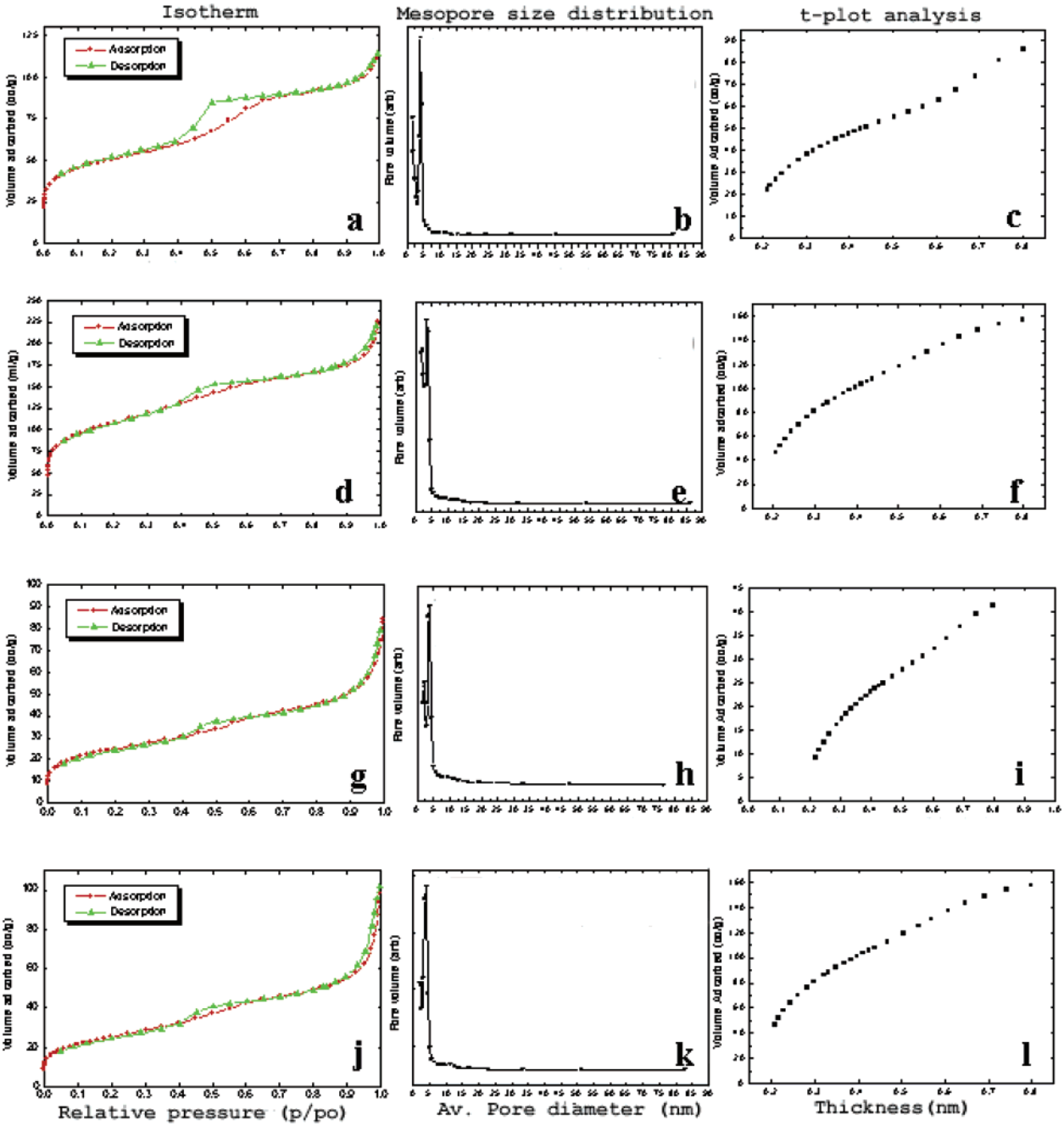

Figure 10. N_2 adsorption data of various calcined samples: (a, b, and c) 1B, (d, e, and f) 2B, (g, h and i) 4B, and (j, k, and l) 5B.

the presence of microporosity. The micropores are certainly disordered, evidenced by the absence of high-angle XRD peaks. The mesopore size distribution and *t*-plots of various samples are also presented in Figure

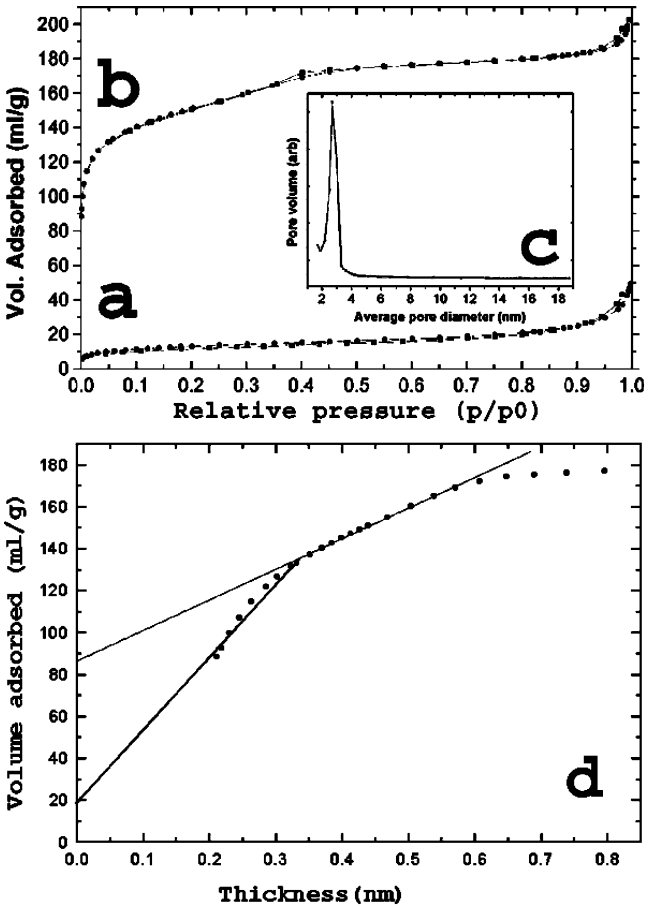

Figure 11. N_2 adsorption isotherm (a: calcined, b: toluene extracted and calcined), desorption pore size distribution (c: toluene extracted and calcined), and t-plot analysis (d: toluene extracted and caclined) of sample 3B.

10. A narrow pore size distribution was observed in all materials with pore size in the range of 3−8 nm. The wall thickness was calculated by subtracting the pore size (d_{mp}) from the unit cell value (d_{XRD}) or repeat distance from TEM images. It is seen that the BET surface area is directly related to the thickness of both macro- and mesostructure. For example, macropore (SEM, Table 3) and mesopore wall thickness ($d_{XRD}-d_{mp}$) of 3B/calcined and 3B/toluene/calcined are 90 and 2 nm and 120 and 5 nm, respectively. The surface area and mesopore volume of these two materials are 46 m^2/g and 0.05 mL/g and 531 m^2/g and 0.19 mL/g (see Table 3). Most of the calcined samples exhibited a poor microporous surface area (Table 3). The heat generated during the melting and burning of a large amount of polystyrene latex inhibited the formation of micropores whereas it is facilitated by initial extraction of polystyrene latex by toluene.

The various Si environments Q^n {where Q^n represents $Si(OSi)_n(OH)_{4-n}$ and $4 \geq n \geq 1$)} can be identified due to the distinct chemical shift values in the ^{29}Si single-pulse MAS NMR spectrum. All samples exhibited a broad ^{29}Si NMR signal (see Supporting Information) in the region −100 to −120 ppm with a center peak at −110 ppm. This broad signal is mostly due to Q^3(Si) and Q^4(Si) sites. The uncalcined sample exhibited both Q^3-(Si) and Q^4(Si) sites. The ratio of the intensity of Q^3(Si) to Q^4(Si) sites decreases with increasing the calcination temperature. The final calcined material (550 °C) exhibited a broad spectrum due to Q^4(Si) sites. The Q^3-(Si) sites were formed while drying the monolith in the presence of silica gel but converted to Q^4(Si) sites during calcination. The ratio of Q^3(Si) to Q^4(Si) of the uncalcined sample remain unchanged during the toluene extraction. The Q^3(Si) species transform to Q^4(Si) species during calcination due to dehydration of neighboring Q^3-(Si) sites. The presence of more Q^3(Si) in 6B/toluene/calcined supports the stability and high surface area of the 6B/toluene/calcined material.

Possible Formation Mechanism. The formation of macrospheres, interconnecting windows, mesopores, and micropores are depicted in Figure 12. The macrospheres are formed due to the removal of polystyrene latex spheres from the monolith. The size of the macrospheres is slightly less than the size of the original polystyrene latex spheres (blue). This is because of shrinkage of silica walls due to melting of polystyrene latex. The formation of mesopores can be explained as follows: The surfactant triblock copolymer Pluronic F127 or P123 contain a chain of ethylene oxide−propylene oxide−ethylene oxide ($EO_{107}PO_{70}EO_{107}$ for F127 and $EO_{20}PO_{70}$-EO_{20} for P123). The polypropylene oxide chains (PPO) are hydrophobic in nature and poly(ethylene oxide) chains (PEO) are hydrophilic in nature. In the presence of water, the surfactants form a micelle where PPO chains stay in the core of the micelle (green) and PEO chains stay in water around the core (red). The size of such a micellar core is around 80 Å (green) and the size of the whole micelle is around 180 Å (see Figure 12).[19] TMOS in an acidic medium is hydrolyzed into cationic silicate species and stays homogeneous in the acidic aqueous solution in the presence of micelles. The silicate−micellar solution diffuses into the interstitial voids of polystyrene monoliths. The diffusion of silicate species into the voids of polystyrene monoliths may be due to the attractive interaction between cationic silicate species with anionic surface charges. The silica−micellar solution finally precipitates around the polystyrene spheres. There is a region where polystyrene monoliths touch each other. There is not enough space for micelles (size restriction) to diffuse near to the touching point

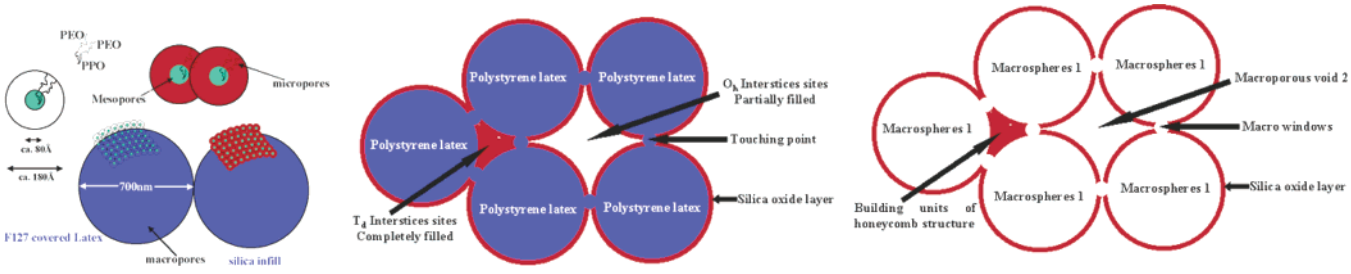

Figure 12. Diagrammatical presentation of the formation of macro−meso−micropores.

whereas small silicate species can easily diffuse around the touching points. Upon removal of polystyrene spheres by solvent extraction or calcination, the macro windows are formed at the touching points of the close-packed latex monolith. The amorphous regions around the windows (see Figure 7) are formed due to the condensation of silicate species without the presence of any micelles. The mesopores are filled with PPO chains of the block copolymer and do not dissolve out by solvent extraction. The core of the micelles can only be removed by heating at 450 °C in the presence of air. The mesopores are formed due to the removal of PPO chains from the core of the micelles and the walls of the mesopores are formed by micropores due to the removal of PEO chains. The micropores are interconnected with mesopores and are disordered. The presence of such a microporous corona[19] or disordered microporosity[20] in mesoporous material synthesized by a similar surfactant was reported recently.

Conclusions

Hierarchically ordered porous silica composites with pore sizes ranging from sub-nanometer to micrometer were synthesized using polystyrene latex and triblock copolymer as templates in the presence of cosurfactants (*n*-alcohol). The macropores (200−800 nm) are well-ordered and interconnected through windows. The window sizes were well-controlled in the range 70−140 nm. The mesoporosity in the hierarchically ordered structure was controlled either by changing the surfactant (triblock copolymer F127/P123) or cosurfactants (*n*-pentanol/*n*-butanol). The F127 surfactant produces ordered mesophases with a hole structure in the presence of *n*-butanol as a cosurfactant whereas a layered structure is produced in the presence of *n*-pentanol as a cosurfactant. The P123 surfactant only produces a layered mesophase in the presence of both cosurfactants. The walls of the mesopores are thick and form with disordered micropores. The surface area of such materials is largely improved when the polystyrene spheres were removed by toluene extraction followed by calcination. The high surface area is due to the equal contribution of both micro- and mesoporosity. Ordering at various length scales with interconnecting macro−meso−micropores and narrow mesopore size distribution makes these materials unique.

Acknowledgment. Thanks to Dr. N. Hanif and Dr. C. C. Egger for running the SEM and TEM and to ICI-Synetix for financial support.

Supporting Information Available: Additional figures (PDF). This material is available free of charge via the Internet at http://pubs.acs.org.

CM034946U

(19) Imperor-Clerc, M.; Davidson, P.; Davidson, A. *J. Am. Chem. Soc.* **2000**, *122*, 11925.
(20) Ryoo, R.; Ko, C. H.; Kruk, M.; Antochshuk, V.; Jaroniec, M. *J. Phys. Chem. B* **2000**, *104*, 11465.